

Article

Synergistic Path for Dual Anisotropic and Electrically Switchable Emission From a Nanocomposite of CsPbBr₃ Quantum Cuboids and Nematic Liquid Crystal

Pragnya Satapathy ^{1,2}, Pralay K. Santra ¹  and S. Krishna Prasad ^{1,*} ¹ Centre for Nano and Soft Matter Sciences, Bengaluru 560013, India² Department of Physics, Mangalore University, Mangalagangotri 574199, India

* Correspondence: skpras@gmail.com

Received: 4 July 2019; Accepted: 20 July 2019; Published: 24 July 2019



Abstract: We report photophysical properties of a nanocomposite consisting of perovskite quantum cuboids (QCs) formed by CsPbBr₃ and a wide temperature range nematic liquid crystal. Contrary to observations made with conventional II-VI quantum dots dispersed in a liquid crystal, the used QCs form, under the influence of the nematic orientation, linear assemblies over macroscopic length scales evidenced by polarizing optical microscopy. Interestingly, the linear assembly is actually caused by such an anisotropic arrangement at the nm scale, as seen in TEM images. Thin films of the nanocomposite exhibiting this unique and fascinating character exhibit absorption and emission features, which are quite appealing. These include retention of the sharp bandwidth of emission characteristic of the native QCs and establishment of dual anisotropies, arising from the values being different along the director as well in the two directions orthogonal to it. We also present data on voltage-driven switching between one of the anisotropic limits.

Keywords: CsPbBr₃ perovskite quantum cuboids; nanocomposites; dual anisotropy; switchable emission; nematic liquid crystals; linear assemblies

1. Introduction

Recently, investigations on composites comprising nanostructures and liquid crystals have become a hot topic owing to the possible complementary aspects in the properties of the two constituents. Liquid crystals (LCs), composed of calamitic, disc-like or banana-shaped molecules, are fluids at least in one dimension, and can exhibit various degrees of ordering that can be tuned by different external control parameters [1]. In the calamitic systems the long axes of the rod-shaped molecules align along a preferred direction, denoted as the director (**n**). The nematic phase, the least ordered LC phase, exhibits long-range orientational order (along **n**), without any positional order. The orientational order brings in anisotropic character to many physical properties, including electrical and optical characteristics, of the medium. For example, the system exhibits finite birefringence, $\Delta n = n_e - n_o$, with n_e and n_o being the extraordinary and ordinary indices of refraction, respectively. While LCs are ubiquitous in flat panel displays, other potential applications for which these materials have assumed significance are waveguiding, beam steering etc. [2]. The ensuing electro-optic behavior forms the basis of LC displays. Owing to the inherent nature of the material, these devices are passive in that they manipulate light falling on them, but do not emit any light of their own. This demands that but for the simple alphanumeric devices, a backlighting is required. While compact fluorescent tubes have been the standard backlighting sources, in recent times, light emitting diodes and quantum dots are taking over. However, it would be quite attractive if the liquid crystal were itself an emitter.

There have been many attempts in this regard. The primary aim of this article is to look at various aspects of photoluminescence (PL) that arises, from a nanocomposite having cesium lead halide perovskite quantum dots incorporated into the liquid crystal medium, keeping in mind anisotropy and switchability of emission.

Quantum dots (QDs) are nanometer-size semiconductor materials with distinctive optical properties determined by their size. Nanoparticles formed by the II-VI group of elements such as CdS and CdSe have been the traditional QDs. These have been superseded by the organic/inorganic hybrid perovskites with the generic formula MAPbX_3 ($\text{MA} = \text{CH}_3\text{NH}_3$; $\text{X} = \text{Cl, Br, I}$), owing to high photoluminescence (PL) quantum yield, low processing temperatures and low cost. However, more recently all inorganic halide perovskite (IHP) QDs, such as CsPbX_3 ($\text{X} = \text{Cl, Br, I}$), are gaining attention from the viewpoint of stability, photovoltaic performances, narrow emission line width and PL efficiency [3,4]; the last of these could easily touch near unity [5]. Nano-soft composites having LC host and a variety of nanostructures playing the role of guests is an upcoming field owing to the complementary nature of the two materials. There have been several studies employing QDs as the nanostructures, and this incorporation leads to lower threshold voltage [6], faster electro-optic response [6] and also moderate emission characteristics [7–9]. It may be pointed out that in all these cases, the QDs used are spherical, unlike IHPs forming cuboids. The latter thus may be anticipated to promote self-assembly into shape anisotropic entities. If the direction of self-assembly can be dictated by external means it would become all the more attractive. With this background we have recently investigated [10] nanocomposites of IHP QDs and an LC host and found that (i) the inherent high PL efficiency of QDs is retained, (ii) QDs do get self-assembled along a direction dictated by the LC host and (iii) that PL exhibits anisotropy between the in-plane and out-of plane directions. In the main results to be presented in this article, we describe further features of this nanocomposite wherein the system exhibits dual absorption and emission anisotropies—out-of-plane as well as within the plane of the equilibrium orientation of the LC molecules—thus establishing the rich variety of PL behaviour.

2. Experimental

CsPbBr_3 quantum cuboids (QCs) were prepared and characterized as described in previous publications [10,11]. In brief, a stock solution of Cs-oleate was prepared Cs_2CO_3 in 1-octadecene (ODE) and oleic acid under alternate cycles of one hour each under vacuum and N_2 atmosphere keeping the temperature constant at 120°C . In a separate three-neck round bottom flask, PbBr_2 was taken in ODE and kept at 120°C under vacuum for 1 hour after which oleic acid and oleylamine were injected. After PbBr_2 got completely dissolved, the reaction temperature was raised to 150°C before quickly injecting the pre-synthesized Cs-oleate, continuing the reaction for 5 seconds and finally quenching in an ice-water bath. To complete the preparation, the wet pellet was dried overnight under vacuum and employed for making mixtures with LC.

The molecular structure of the host calamitic LC compound, 4-pentylphenyl 2-chloro-4-(4-pentyl benzyloxy) benzoate or PCPBB for short, exhibits the nematic phase over a wide-range of temperatures through room temperature and has been used specifically for its dual frequency dielectric feature [12,13]. The composite, hereafter referred to as CsLC mixture, containing 2 wt% of CsPbBr_3 in PCPBB, was prepared using the standard solution-mixing procedure followed by sonication and high-temperature treatment; toluene was used as the solvent for this purpose. Finally, the mixture was placed under vacuum for 5 hours to ensure removal of any traces of toluene. For photoluminescence measurements, cells made of indium tin oxide (ITO) coated glass plates (electrode gap of $\sim 25\ \mu\text{m}$), whose inside surfaces had a rubbed polyimide alignment layer, were employed. Transmission electron microscopy (TEM) images were obtained using TALOS F200S G2 field emission transmission electron microscope (ThermoFisher Scientific, OR, United States) operated at an accelerating voltage of 200 kV. For photoluminescence experiments, a Spectrofluorometer (Fluorolog –3, Horoba Jobin Yvon with a Xenon lamp source) was employed.

3. Results and Discussion

3.1. Microscopy

In our previous report on this topic [10], we demonstrated that in the CsLC nanocomposite the PL magnitude depends on whether the LC molecules are in the plane of the substrate or out of it. We extend this observation further and investigate whether there is anisotropy of PL in the plane itself. For this purpose, we define the coordinate system as shown in Figure 1a. The plane formed by the substrates, also containing the LC director (\mathbf{n}) under equilibrium conditions, is taken to be the XY plane. The rubbing direction of the polyimide layer, which fixes the orientation direction of the employed calamitic LC molecules is denoted as X, and the direction orthogonal to it, but in the plane, as Y. The Z direction is normal to the XY plane and is also the direction along which the electric field gets applied to obtain reorientation of the molecules. With this background, let us first look at the TEM images. The as-prepared CsPbBr₃ nanoparticles are seen to be cuboids (Figure 1b) with an edge length of 13.7 ± 3.1 nm. As detailed out in [10], XRD data confirm the orthorhombic crystal structure. Of specific interest from the viewpoint of current studies is the influence of LC orientation on the disposition of the quantum cuboids. The TEM image obtained from the CsLC mixture is shown in Figure 1c, exhibiting a linear assembly. In fact, QCs get organized along their body diagonals as seen in the HRTEM image (Figure 1d) and schematically sketched in Figure 1e. As stated earlier the QCs line-up along the LC director (X direction). A point that may be emphasized is that QCs do fuse to achieve a directed overlap while forming linear assemblies. It is argued [10] that a few of the ligands decorating the QCs may be getting substituted by the LC molecules, which generates a continuity with the neighbouring nematogens and consequently favours a tendency to align along the director.

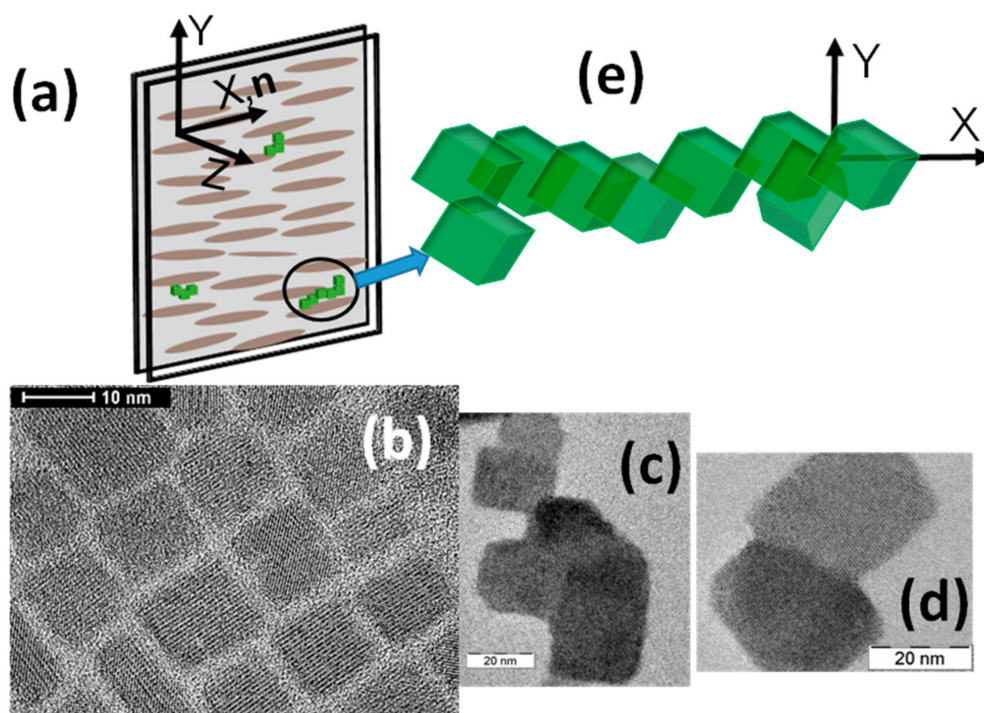


Figure 1. TEM images of (a) the as-synthesized CsPbBr₃ quantum dots exhibiting cuboidal architecture. When dispersed in the nematic LC, the neighbouring cuboids organize along their body diagonal (see images b and c) and develop a tendency to form linear assemblies along the director direction, schematically shown in (d); the TEM images are adapted from [10].

The linear superstructure seen in TEM images actually manifests on truly macroscopic scales, as seen in the POM studies. For this purpose, a thin film of the CsLC sample was placed between two glass

substrates whose inner surfaces were treated with a polyimide layer that promotes planar orientation of the LC molecules. POM observations made without the analyzer to avoid the birefringence influence showed that the QCs are generally aligned along the director over regions as large as a few hundred microns (Figure 2a). The self-assembly is evident when the microscope white light source was replaced by the QC-exciting blue light from a laser diode having a wavelength of 404 nm (Figure 2b). In fact, independent observations made with the traditional QDs made of II-VI semiconductors do not show such linear self-assembly [14]. Thus, the self-assembly in the CsLC system, which is unprecedented in LC-QD composites can pave way for new kinds of structures that will allow for the anisotropic PL as the superstructure has a non-isotropic feature.

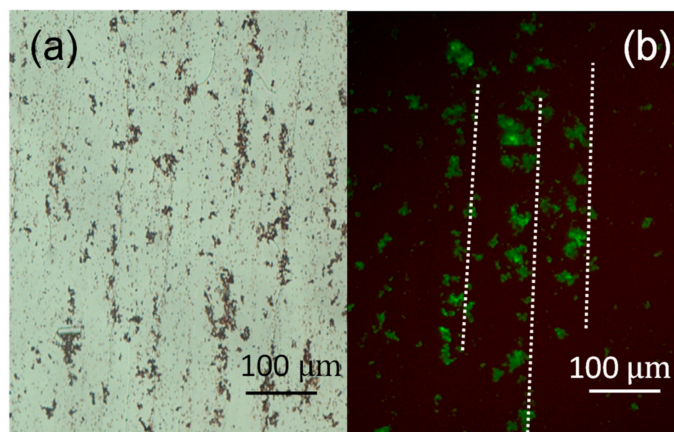


Figure 2. Polarizing optical microscopy (POM) images in the nematic phase of CsLC at 30 °C captured with (a) white light and (b) excitation light obtained from a 404 nm laser. The linear assembly of QCs along the director direction \mathbf{n} is seen as dark objects on the grey nematic background for white light and bright green regions for 404 nm excitation. The influence of LC birefringence was avoided by removing the analyzer.

3.2. Absorption

In core/shell CdSe/CdS nanostructures, by encapsulating wurtzite QD cores within an anisotropic shell large, positive optical anisotropy has been realized [15]. Anisotropic emission has also been used in CsPbX₃ QCs with the anisotropy being the largest when iodine is employed as the halide [16]. In our previous work [10], we showed that anisotropy could also be achieved by dispersing CsPbX₃ QCs in a liquid crystal host. Observing an unprecedented LC-driven linear assembly of these QCs, and relying on the inherent property of LC molecules to get reoriented from the surface-dictated orientation to field-dictated direction, the X-Z anisotropy was proved. In this case, the photoselection was done with a horizontal (H) polarizer parallel to the X axis; this allowed to selectively excite QC assembly aligned with the polarization of the excitation source. Through optical microscopy studies, it was also seen that when the applied electric field reorients the LC molecules to be along the Z (out-of-plane) direction, some of the QCs (or QC assemblies) do get reoriented perhaps due to sympathetic communication between the LCs and QCs. Barring such entities, a large number of QCs continue to remain along the X axis even after the LC reorientation. Extending these measurements, we now establish that there is indeed anisotropy in the (XY) plane containing the LC molecules in the equilibrium (no-field) state. To obtain data along the second in-plane direction Y the sample cell was rotated about the incoming beam axis such that the LC orientation direction (X) is normal to the polarizer direction that was kept fixed. A schematic representation of these two geometries is presented in Figure 3 and the corresponding absorption spectra are shown in Figure 4a. The absorption profiles appear qualitatively similar for the two orientations but with substantial difference in the absolute values, the magnitude being larger for the X direction. This difference is significant in comparison with that obtained between the X and Z directions, the latter, also being shown in Figure 4a, achieved by electrical switching of the LC

molecules. The temperature dependence of the absorbance values A_n ($n = X, Y$ or Z) for the different directions obtained at a wavelength of 404 nm are shown in Figure 4b; at all temperatures the relation $A_X > A_Z > A_Y$ is seen to be true.

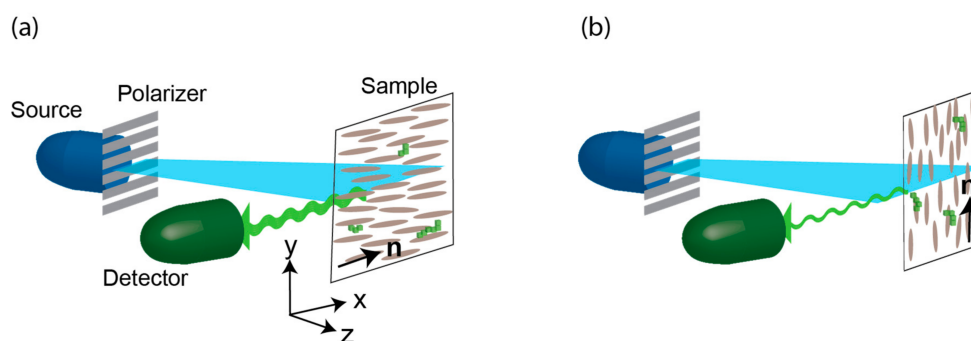


Figure 3. Schematic representation of the geometries employed to obtain X-Y anisotropic emission depicting the liquid crystal alignment and polarization of the incident light whose direction is decided by the polarizer oriented horizontally. The arrangement is referred to as X when the director is parallel to this horizontal (panel a), as Y when the director is perpendicular but still in the substrate plane (panel b), and as Z when the director becomes out of plane. In the sample plane, the ellipses represent LC molecules, and the blocks QC assembly.

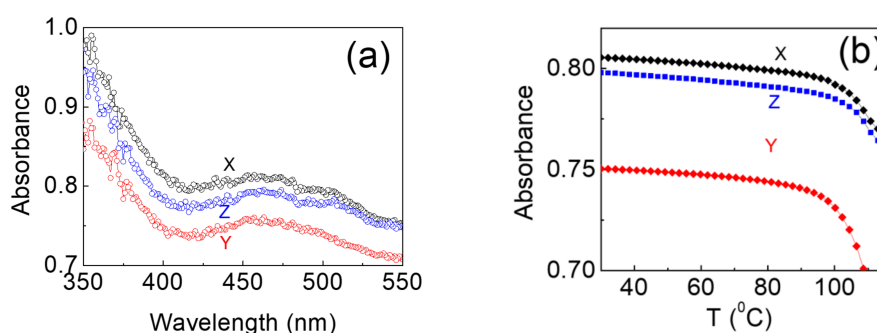


Figure 4. (a) Spectra of A_X , A_Y and A_Z , the absorbances for the three directions, X, Y and Z. To be noted is that the difference is substantial between A_X and A_Y , and less so between A_X and A_Z . (b) Temperature dependence of A_X , A_Y and A_Z at 404 nm. Interestingly in the vicinity of the N-I transition, A_Y shows a much larger variation than the other two parameters.

This is surprising since from the host liquid crystal point of view, another optical parameter viz., the refractive index has only two values, the ordinary n_o and the extraordinary n_e . For the incoming light, n_e would be along X, and owing to the cylindrical symmetry of the system, both Y and Z would be equivalent with n_o as the refractive index. Thus, $A_Z \neq A_Y$ is surprising. In all cases, away from T_{NI} , the nematic-isotropic transition temperature, the absorbance decreases weakly on temperature, but closer to it, the behavior depends on the direction. While A_X and A_Z have similar and small decrease, A_Y has a large reduction becoming almost immeasurable in the immediate vicinity of T_{NI} . Thus, we define two anisotropic absorptions $\Delta A_{XY} = (A_X - A_Y) / (A_X + 2A_Y)$ and $\Delta A_{XZ} = (A_X - A_Z) / (A_X + 2A_Z)$, with the form of the denominator indicating the anisotropic average of the involved absorptions. Figure 5 presents the temperature dependence of ΔA_{XY} and ΔA_{XZ} . The first thing to note is that ΔA_{XY} is an order of magnitude larger than ΔA_{XZ} . Secondly, the two anisotropies have opposite temperature dependence: While ΔA_{XY} is hardly dependent on temperature at lower temperatures, but on approaching T_{NI} shows a drastic increase. In contrast, ΔA_{XZ} weakly increases with temperature at lower temperatures, reverse its trend and precipitously drops near T_{NI} . The trend seen for ΔA_{XZ} near the transition is typical of the behavior of the order parameter, such as, for example, the optical anisotropy or the birefringence. Owing to the similarity in the behavior, it is tempting to suggest that ΔA_{XZ} is the order parameter for the system. However, the increasing trend seen on approaching T_{NI} ,

rules out a similar assignment for ΔA_{XY} . Now, let us consider the following. The absorbance gets contribution from the nematic ordering besides that by the QCs. Thus, the total absorption A can be represented as

$$A = \varphi_1 n_{QC} + \varphi_2 n_{LC} \quad (1)$$

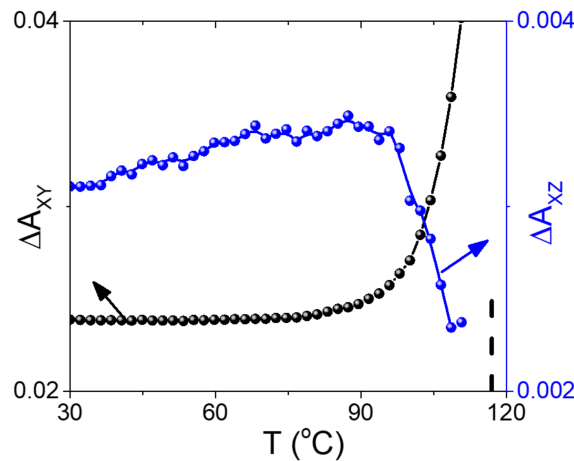


Figure 5. Thermal variation of the two absorption anisotropies, ΔA_{XY} and ΔA_{XZ} . The in-plane anisotropy ΔA_{XY} is about an order of magnitude larger than ΔA_{XZ} . The two anisotropies have opposite temperature dependence, ΔA_{XY} increasing and decreasing on approaching T_{NI} (marked as the vertical dash line).

Here φ_1 and φ_2 are prefactors, n_{QC} and n_{LC} are the refractive indices of CsPbBr_3 and the LC. n_{LC} is known to be anisotropic and thus its value could be either n_e or n_o depending on the polarization of incident light with respect to the orientation direction of the LC molecules. Determined by the self-assembly at the nm (Figure 1) as well as at the μm scale (Figure 2), A_X is dominated by the contribution from QCs. It is known that the difference in refractive index between an anisotropic nanostructure and its environment renders substantial end facet reflectivity [17]. Since the LC medium, which surrounds QCs, is also anisotropic, in the present case the environmental influence is also direction-dependent. Thus, the observed anisotropic absorption could be explained by the environmental effect. However, as ΔA_{XY} and ΔA_{XZ} are significantly different, we treat eq. (1) to be direction-dependent and express this feature as

$$A_X = \varphi_1 n_{QC} + \varphi_2 n_e \quad (2)$$

$$A_Y = \varphi_3 n_{QC} + \varphi_2 n_o \quad (3)$$

$$A_Z = \varphi_1 n_{QC} + \varphi_2 n_o \quad (4)$$

Considering that the absorptions measured in both the Y and Z directions are lower than that for the X direction, we take the second term in each of the expressions (2)–(4) to have a subtractive effect on the first term, and φ_1 , φ_2 , φ_3 are < 1 . It may be noted that in this formalism, since during the electric field-driven reorientation of LCs, a majority of QCs are not seen to be rotating with the LC, the first term remains identical for A_X and A_Z . Thus, ΔA_{XZ} would be given by the product of φ_2 and birefringence ($n_e - n_o$), which has a value of ~ 0.1 for the LC used here with n_{QC} taken as 2.2 [18]. With these considerations, we work out φ_1 , φ_2 , φ_3 to be 0.3, 0.1 and 0.4. Hence, ΔA_{XY} would be more dominating than ΔA_{XZ} . A possible reason for the inequality of φ_1 and φ_3 could have its origin in the anisotropic absorption expected and observed in shape anisotropic quantum nanostructures [18,19]. These arguments fit very well with the considerations that colloidal nanorods behave like miniature bar polarizers, selectively attenuating incident electric fields polarized orthogonal to their long axes [20].

Thus, in the Y configuration, the linear assembly of the QCs, which may be loosely defined as nanorods, can be expected to attenuate light polarized along the X axis. In fact, the authors of Ref. [21] compute the absorption anisotropy of a system of CdSe/CdS nanorods embedded in a dielectric medium in terms of $\frac{\epsilon_{\text{medium}}}{(1-\alpha)\epsilon_{\text{medium}}} - \epsilon_{\text{rod}}$, where α is the depolarization factor, lending support to the equations (2)–(4) that we have proposed.

3.3. Dual Anisotropic Photoluminescence

The photoluminescence (PL) spectra obtained with 404 nm excitation of the CsLC nanocomposite in the X, Y and Z configurations are shown in Figure 6a. The peak emission wavelength is unaltered in all these cases, but peak magnitude (I_{em}) follows the relation $I_X > I_Z > I_Y$, just as expected from the absorption data. The temperature dependences of these parameters (Figure 6b) show that over the entire thermal range of the nematic, this relation remains true. We calculate the ΔI_{XY} and ΔI_{XZ} the two anisotropies in emission using the expression [21].

$$\Delta I_{XY} = (I_X - I_Y) / (I_X + 2I_Y) \quad (5)$$

$$\Delta I_{XZ} = (I_X - I_Z) / (I_X + 2I_Z) \quad (6)$$

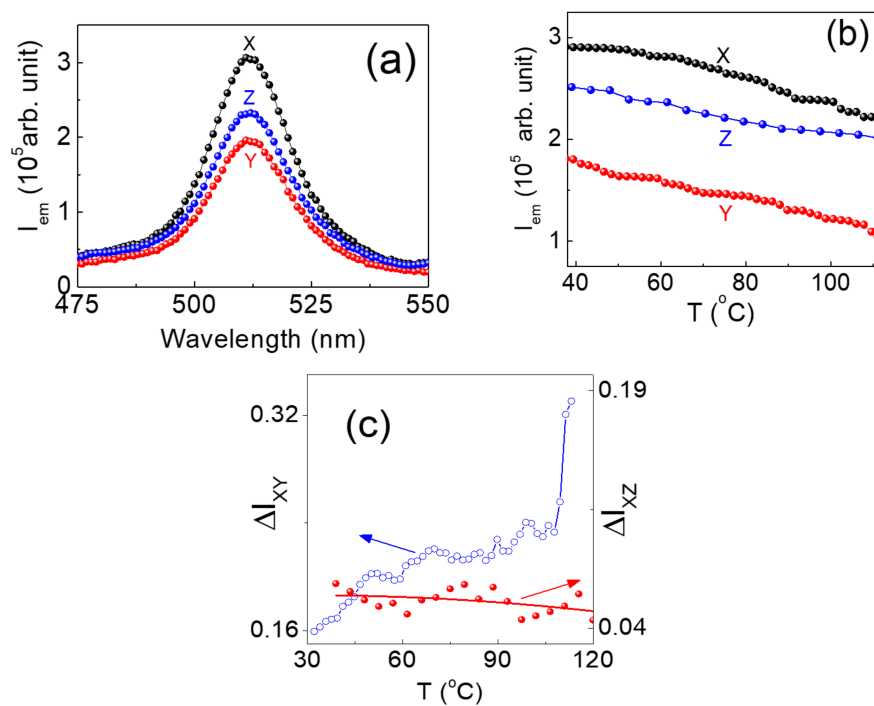


Figure 6. (a) Photoluminescence spectra at room temperature obtained with excitation at 404 nm for a thin film of the CsLC nanocomposite in the X, Y and Z geometries described in Figure 3. While the wavelength of peak emission remains the same, the magnitude varies with the geometry. (b) Thermal variations of the peak emissions I_X , I_Y and I_Z , exhibiting a similar relation as the corresponding absorptions A_X , A_Y and A_Z . (c) Influence of temperature on ΔI_{XY} and ΔI_{XZ} , the two anisotropies of emission, as calculated using Equations (5) and (6).

The thermal variations of these anisotropies are depicted in Figure 6c, and exhibit, interestingly but not surprisingly, behavior quite similar to the corresponding absorption anisotropies: ΔI_{XY} increases whereas ΔI_{XZ} diminishes on approaching T_{NI} . The fact that the individual I_{em} still have a decreasing trend as temperature is raised (see Figure 6b) suggests that the polarization discrimination mentioned above is better in the vicinity of T_{NI} , a feature that is counterintuitive, and the reason for which is not clear to us.

3.4. Voltage-Switchable Photoluminescence

It has been mentioned above that the LC molecules can be made to switch from the equilibrium X to the Z direction to be along the applied field. This is based on the well-known Fredericksz transformation phenomenon, involving application of an ac electric field having a frequency lower than the director relaxation frequency, and a voltage (V) above a threshold voltage (V_{th}). The molecular reorientation gets initiated at V_{th} , and for $V > V_{th}$ the molecules become normal to the substrate. The PL spectra obtained at room temperature for different voltages in the range of 0 to 18 V_{rms} and at a fixed frequency of 1 kHz, covering the reorientation of molecules from the X (0 V) to Z (18 V) direction, are shown in Figure 7a. As already seen in Figure 6a, at all voltages, the peak emission wavelength remains unaltered. The peak emission level is plotted as a function of voltage in Figure 7b, and presents a behaviour standard for threshold-operated parameters. The threshold voltage is determined to be 5.5 V, a value that is higher than that obtained with permittivity data, which are treated as a direct measure of the reorientation. The dynamic response of the system switching between these two anisotropic limits for voltage ON (18 V) and voltage OFF (0 V) cases, is depicted in Figure 7c showing that the switching is quite rapid, although has a significant tail region for the switch-off process. We have previously [10] shown that owing to the dual frequency capability of the LC host, instead of switching the voltage off, the frequency of the field can be made high (~ 50 kHz) to realize fast (1 ms) responses from the system. Our preliminary measurements show that ΔI_{XY} remains quite high over the studied 0–20 V range. If field-driven operation is possible for the X-Y switching also, it would result in large voltage-controlled fluorescence swings. While the magnitude of PL swing is much larger than for the X-Z switching, the response is thresholdless, as it should be. We are in the process of realizing the proper geometry needed for the purpose.

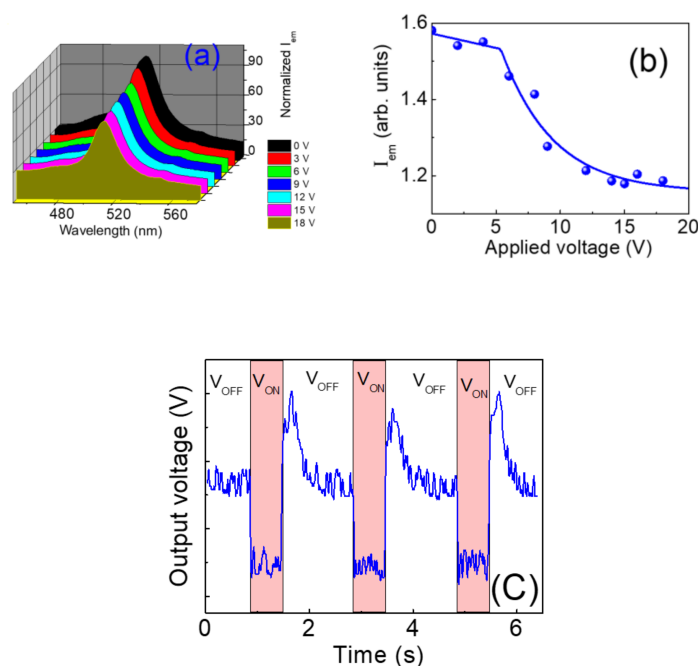


Figure 7. (a) Photoluminescence spectra obtained at room temperature with different applied voltages in the range 0 to 18 V, with the 0 V profile representing the equilibrium planar orientation of the LC molecules with the director parallel to X direction, and the higher voltage profiles approaching the asymptotic situation of homeotropic orientation where the director is parallel to the Z direction. (b) Voltage dependence of the peak emission magnitude exhibiting a clear threshold ~ 6 V and a limiting behaviour at the highest voltage. (c) Dynamics response of the PL switching at room temperature when the voltage (20 V, 1 kHz sinewave) is turned on and subsequently off.

4. Summary and Outlook

We have described photophysical properties in a nanocomposite comprising cesium lead halide perovskite quantum cuboids (QCs) dispersed in a wide temperature range nematic liquid crystal. Unlike the liquid crystal systems composed of conventional II-VI quantum dots, the QCs employed here exhibit linear assemblies clearly seen at the nm scale, through TEM, and at the mm scale, through polarizing optical microscope. Such linear superstructures are all the more attractive since the assembly is directed to be along the nematic director. Employing such assemblies we demonstrate several interesting features including (i) unaltered bandwidth of emission, which retains the same sharpness as the native QCs, (ii) dual anisotropies, brought about by values being different along all the three directions with reference to the director, (iii) voltage-driven switching between anisotropic limits and (iv) fast field-driven response. These investigations are being extended at several levels, some of which are indicated in the following.

The ligands that cover the QCs are, by design, organic in nature. From the viewpoint of stabilizing larger concentration of QCs, it would be advantageous to use mesogenic entities to take the place of the ligands. Such ligands, when properly incorporated, not only provide better compatibility between the inorganic and organic environments but will offer a variety of liquid crystalline structures, which can enrich the field of QC-LC nanocomposites. Chirality of the constituents plays an important role in discriminating and even amplifying light having specific circular polarization. While the molecular chirality of the ligands is the basis, the self assembly such as the ones discussed in this article could lead to structural chirality and consequently chiral amplification. Obviously, this scheme presents development of materials that can be generating both left handed and right handed circularly polarized light. A further extension would be to associate QCs with LC photonic structures exhibited by chiral nematic, twist grain boundary and Blue phases. For example, the chiral nematic or cholesteric phase displays photonic band gap (PBG) due to the presence of a helical structure present normal to the local director direction. If light is propagating along the helical axis, then the pitch p of the helix is given by $\lambda_0 \cdot n_{\text{avg}}$, λ_0 being the wavelength of the maximum reflection and n_{avg} , the average of n_e and n_o ; $p \cdot \Delta n$ defines the width of PBG. In recent times there has been much activity to achieve materials with desired characteristics of PBG: λ_0 in the vis/NIR, improved bandwidth and enhanced reflection. A more recent addition has been to include PL functionality, and will have much impact on new generation optical devices such as in reflective displays with high contrast ratio and distributed feedback lasers. The helix of cholesteric LCs acts as a selective absorber of wavelengths determined by PBG. A potentially better PL system can thus be designed by synergistically appealing to the characteristics of the PL and PBG materials. In fact, we have recently demonstrated that large enhancement in emission can be achieved by matching the excitation wavelength λ_{ex} of the PL material with the selective absorption wavelength λ_0 of the PBG material [22]. Replacing the organic emitter used in this case by QCs would thus be a path to achieve narrow bandwidth emissions amplified by the PBG structure.

Another dimension for CsLC nanocomposites that we are working is towards optical control of QC emission. The optical control is through photoisomerization of photoactive molecules such as azobenzene, which upon irradiation with actinic light undergo shape transformation from rod-like to bent-form [23,24]. This shape transformation is known to have a strong effect on the LC and its properties. Preliminary measurements performed on a LC-quantum dot composite in which an azobenzene derivative is physically mixed (for a schematic representation of the situation see Figure 8a shows promising results. We are working towards quantum dots which are decorated with photoactive ligands, and form a dimer, trimer or other such n -mer entities (see Figure 8b). Forward and reverse photoisomerization of the ligands should then lead to a “breathing” response from the quantum dot n -mers varying the super-particle size. Through proper design this would manipulate the energy transfer allowing for optical control of emission wavelength.

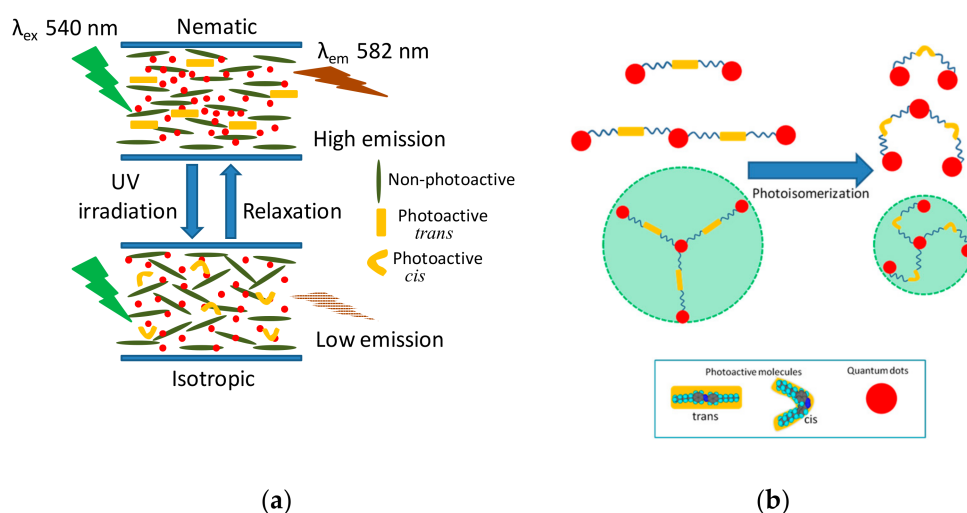


Figure 8. (a) Schematic representation of optically driving the fluorescence change from high to low values. The azobenzene derivative responsible for this has an equilibrium rod-shaped trans state, which upon photoisomerization changes to bent cis state. This change in shape of the minority azobenzene molecules drives the entire system isothermally from the nematic to the isotropic phase. Through different pathways the system returns to the trans isomer of azobenzene, and the equilibrium nematic phase. (b) Chemically bound azobenzene and quantum dot system in (i) dimer, (ii) trimer and (iii) star-shaped forms in the equilibrium and photoisomerized states. To be noticed is the size reduction/shape change of the assembly during the process.

Author Contributions: Performing experiments and formal analysis, P.S.; providing quantum cuboids and information on their basic characterization, P.K.S.; supervision and experimental designing, S.K.P.

Funding: This research was funded by DST, New Delhi, India, grant number SR/NM/TP-2 5/2016.

Acknowledgments: Project-specific financial support as well as the TEM facility funded by the Thematic project (SR/NM/TP-2 5/2016), Nano Mission, DST, New Delhi, India, is gratefully acknowledged. PS thanks DST Inspire for a fellowship.

Conflicts of Interest: The authors declare no conflict of interest.

References

- Chandrasekhar, S. *Liquid Crystals*, 2nd ed.; Cambridge University Press: Cambridge, UK, 1992.
- He, Z.; Gou, F.; Chen, R.; Yin, K.; Zhan, T.; Wu, S.-T. Liquid Crystal Beam Steering Devices: Principles, Recent Advances, and Future Developments. *Crystal* **2019**, *9*, 292. [[CrossRef](#)]
- Tang, X.; Zu, Z.; Shao, H.; Hu, W.; Zhou, M.; Deng, M.; Chen, W.; Zang, Z.; Zhua, T.; Xue, J. All-inorganic perovskite CsPb(Br/I)₃ nanorods for optoelectronic application. *Nanoscale* **2016**, *8*, 15158–15161. [[CrossRef](#)] [[PubMed](#)]
- Chuang, C.H.; Brown, P.R.; Bulović, V.; Bawendi, M.G. Improved performance and stability in quantum dot solar cells through band alignment engineering. *Nat. Mater.* **2014**, *13*, 796–801. [[CrossRef](#)] [[PubMed](#)]
- Liu, R.-S. *Phosphors, Up Conversion Nano Particles, Quantum Dots and Their Applications*; Springer: Berlin/Heidelberg, Germany, 2016; Volume 1.
- Anczykowska, A.; Bartkiewicz, S.; Nyk, M.; Mysliwiec, J. Study of Semiconductor Quantum Dots Influence on Photorefractivity of Liquid Crystals. *Appl. Phys. Lett.* **2012**, *101*, 101107. [[CrossRef](#)]
- Dong, Y.; Qiao, T.; Kim, D.; Parobek, D.; Rossi, D.; Son, D.H. Precise Control of Quantum Confinement in Cesium Lead Halide Perovskite Quantum Dots via Thermodynamic Equilibrium. *Nano Lett.* **2018**, *18*, 3716–3722. [[CrossRef](#)] [[PubMed](#)]
- Li, J.; Xu, L.; Wang, T.; Song, J.; Chen, J.; Xue, J.; Dong, Y.; Cai, B.; Shan, Q.; Han, B.; et al. 50-Fold EQE Improvement up to 6.27% of Solution-Processed All-Inorganic Perovskite CsPbBr₃ QLEDs via Surface Ligand Density Control. *Adv. Mater.* **2017**, *29*, 1603885. [[CrossRef](#)] [[PubMed](#)]

9. Singh, G.; Fisch, M.R.; Kumar, S. Tunable Polarised Fluorescence of Quantum Dot Doped Nematic Liquid Crystals. *Liq. Cryst.* **2017**, *44*, 444–452. [[CrossRef](#)]
10. Satapathy, P.; Santra, P.K.; Haque, A.; Yelamaggad, C.V.; Das, S.; Prasad, S.K. Anisotropic Fast Electrically Switchable Emission from Composites of CsPbBr₃ Perovskite Quantum Cuboids in a Nematic Liquid Crystal. *Adv. Opt. Mater.* **2019**, *7*, 1801408. [[CrossRef](#)]
11. Kim, Y.; Yassitepe, E.; Voznyy, O.; Comin, R.; Walters, G.; Gong, X.; Kanjanaboos, P.; Nogueira, A.F.; Sargent, E.H. Efficient Luminescence from Perovskite Quantum Dot Solids. *ACS Appl. Mater. Interfaces* **2015**, *7*, 25007–25013. [[CrossRef](#)] [[PubMed](#)]
12. Hegde, G.; Nair, G.G.; Prasad, S.K.; Yelamaggad, C.V. A Photodriven Dual-Frequency Addressable Optical Device. *J. Appl. Phys.* **2005**, *97*, 93105. [[CrossRef](#)]
13. Madhuri, P.L.; Rao, D.S.S.; Yelamaggad, C.V.; Achalkumar, A.S.; Prasad, S.K. Fast Photoluminescence Switching in the Nematic Phase of Calamitic–Discotic Composites. *Adv. Opt. Mater.* **2015**, *3*, 1116–1124. [[CrossRef](#)]
14. Satapathy, P.; Santra, P.K.; Prasad, S.K. Mangalore University, India. Unpublished work. 2019.
15. Diroll, B.T.; Koschitzky, A.; Murray, C.B. Tunable Optical Anisotropy of Seeded CdSe/CdS Nanorods. *J. Phys. Chem. Lett.* **2014**, *5*, 85–91. [[CrossRef](#)] [[PubMed](#)]
16. Wang, D.; Wu, D.; Dong, D.; Chen, W.; Hao, J.; Qin, J.; Xu, B.; Wang, K.; Sun, X. Polarized Emission from CsPbX₃ Perovskite Quantum Dots. *Nanoscale* **2016**, *8*, 11565–11570. [[CrossRef](#)] [[PubMed](#)]
17. Eaton, S.W.; Lai, M.; Gibson, N.A.; Wong, A.B.; Dou, L.; Ma, J.; Wang, L.-W.; Leone, S.R.; Yang, P. Lasing in Robust Cesium Lead Halide Perovskite Nanowires. *Proc. Natl. Acad. Sci.* **2016**, *113*, 1993–1998. [[CrossRef](#)] [[PubMed](#)]
18. Dirin, D.N.; Cherniukh, I.; Yakunin, S.; Shynkarenko, Y.; Kovalenko, M.V. Solution-Grown CsPbBr₃ Perovskite Single Crystals for Photon Detection. *Chem. Mater.* **2016**, *28*, 8470–8474. [[CrossRef](#)] [[PubMed](#)]
19. Cunningham, P.D.; Boercker, J.E.; Placencia, D.; Tischler, J.G. Anisotropic Absorption in PbSe Nanorods. *ACS Nano* **2014**, *8*, 581–590. [[CrossRef](#)]
20. Dasallas, L.L.; Jaculbia, R.B.; Balois, M.V.; Garcia, W.O.; Hayazawa, N. Position, Orientation, and Relative Quantum Yield Ratio Determination of Fluorescent Nanoemitters via Combined Laser Scanning Microscopy and Polarization Measurements. *Opt. Mater. Express* **2018**, *8*, 1290–1304. [[CrossRef](#)]
21. Diroll, B.T.; Dadosh, T.; Koschitzky, A.; Goldman, Y.E.; Murray, C.B. Interpreting the Energy-Dependent Anisotropy of Colloidal Nanorods Using Ensemble and Single-Particle Spectroscopy. *J. Phys. Chem. C* **2013**, *117*, 23928–23937. [[CrossRef](#)]
22. Baral, M.; Prasad, S.K.; Patel, H.; Achalkumar, A.S.; Yelamaggad, C.V. Giant enhancement of photoluminescence and tertiary emission in a chiral nematic by matching photonic band gap and excitation wavelength. *J. Mol. Liq.* **2018**, *262*, 354–362. [[CrossRef](#)]
23. Prasad, S. K. Photostimulated and photo suppressed phase transitions in liquid crystals. *Angew. Chem. Int. Ed.* **2012**, *51*, 10708. [[CrossRef](#)] [[PubMed](#)]
24. Smart Light-Responsive Materials: Azobenzene-Containing Polymers and Liquid Crystals. Zhao, Y.; Ikeda, T. (Eds.) John Wiley & Sons: Hoboken, NJ, USA, 2009.

